

REVIEW

Open Access



# Development of photocatalytic and electrocatalytic coatings via thermal spraying for environmental and energy storage applications: a short review

Zexin Yu<sup>1,2,3\*</sup>, Botong Wang<sup>3</sup>, Longen Gui<sup>3</sup>, Meimei Liu<sup>4\*</sup>, Shaowu Liu<sup>5\*</sup>, Michel Moliere<sup>2</sup> and Hanlin LIAO<sup>2</sup>

## Abstract

With the development of society, human beings are facing environmental problems and an energy crisis worldwide. In this context, photocatalysis and electrocatalysis represent promising technologies to help solving these issues. Up to now, most of the catalysts intended for these usages are prepared via time-consuming wet-chemical approaches, e.g. hydrothermal or sol-gel methods. Moreover, these techniques produce powdery catalysts which need not only a post-filtration step, but also a shaping by a binder for their final applications, which makes the manufacturing cumbersome. Thermal spraying is currently a well-established deposition technique that is capable of elaborating a wide series of functional coatings based on all classes of materials (metals, polymers, ceramics) and featuring tunable compositions as well as micro- and nanostructures. In particular, thermal involving liquid feedstock, and more specifically precursor solutions or suspensions, have allowed generating a wide range of coating thicknesses, from the ten-micron to the submicron/nano scale, increasing thereby the possibilities for enhancing catalytic performances. The present review sets out marking researches relating to the preparation and testing of (i) some photocatalytic coatings intended for the degradation of aqueous organic pollutants and (ii) electrocatalytic coatings investigated as potential energy storage devices. This paper will not only deal with the preparation of catalysts via different thermal spray processes, but also will cover the adjustment of phase compositions and microstructures that are rendered possible when using liquid feedstock thermal spray techniques with the prospect of optimizing the catalytic performances.

**Keywords** Thermal spraying, Solution precursor plasma spraying, Suspension plasma spraying photocatalytic coatings, Supercapacitor electrode coatings

\*Correspondence:

Zexin Yu  
yu.zexin@ifkb.uni-stuttgart.de  
Meimei Liu  
lmm89zx@163.com  
Shaowu Liu  
shaowuliu93@163.com

<sup>1</sup> Institute for Manufacturing Technologies of Ceramic Components and Composites (IMTCCC), University of Stuttgart, Allmandring 7B, 70569 Stuttgart, Germany

<sup>2</sup> UMR 6303, Site de UTBM, ICB-LERMPCSNRS Université de Bourgogne Franche-Comté, 90010 Belfort, France

<sup>3</sup> School of Mechanical and Electrical Engineering, Soochow University, Suzhou 215123, China

<sup>4</sup> School of Mechanical Engineering, Suzhou University of Science and Technology, Suzhou 215009, China

<sup>5</sup> UMR 8207 - UMET - Unité Matériaux Et Transformations, Univ. Lille, CNRS, INRAE, Centrale Lille, 59000 Lille, France



© The Author(s) 2024. **Open Access** This article is licensed under a Creative Commons Attribution 4.0 International License, which permits use, sharing, adaptation, distribution and reproduction in any medium or format, as long as you give appropriate credit to the original author(s) and the source, provide a link to the Creative Commons licence, and indicate if changes were made. The images or other third party material in this article are included in the article's Creative Commons licence, unless indicated otherwise in a credit line to the material. If material is not included in the article's Creative Commons licence and your intended use is not permitted by statutory regulation or exceeds the permitted use, you will need to obtain permission directly from the copyright holder. To view a copy of this licence, visit <http://creativecommons.org/licenses/by/4.0/>.

## 1 Introduction

The progress realized in the field of thermal spraying are paving the way to new applications which were until now reserved for traditional methods. In this regard, it is worth reporting some recent results obtained by thermally sprayed coatings in the fields of pollutant degradation and energy storage. The first field regards the photocatalytic degradation (PCD) of organic pollutants that are wasted by e.g. the textile industry worldwide [1]. As early as in the 90's, pioneering works have unveiled the photocatalytic degradation (PCD) pathway as a potential water purification technique [2]. As a result, the metal oxide semiconductors (MOS) used in this type of processing, namely  $\text{TiO}_2$  and  $\text{ZnO}$ , became popular photocatalysts for the removal of organic pollutants [3]. The second topic regards new devices that are experiencing rapid development in the storage of electricity. In this area, there is a multiplicity of existing electrochemical systems; among them, Li-ion batteries and supercapacitors are the most investigated devices by researchers. For example, the newly developed supercapacitors possess outstanding advantages due to their high power density and safety level, fast charge and discharge cycles, and long lifetime ( $> 10,000$  cycles) [4, 5].

The optimization of the preparation of photocatalysts and electrocatalysts resorting to conventional synthesis methods is a very active field of research [6–10]. Taking photodegradation catalysts as an example, various conventional techniques, e.g. hydrothermal, solvothermal, sol-gel and co-precipitation, enable adjusting to some extent the morphologies and phase compositions to optimize performances [6]. Regarding more specifically the preparation of electrodes for energy storage, conventional syntheses include also chemical bath deposition, sol-gel, electrophoretic deposition, spin-coating technology [8–10]. However, these methods involve multi-step processes, long preparation times, rather low yields, making them uneasy to industrialize. In addition, these conventional routes produce electrode materials in the form of powders, which requires preparation of slurry, adding organic binders and screen to obtain exploitable electrode coatings [11–15]. The incorporation of such binders in supercapacitor and Li-ion batteries, and their progressive ageing create additional issues in terms of activity and stability. The losses of nanoparticles incurred in these processes are also damageable [16–18] as well as the necessary use of surfactants or templates, such as hexamethylenetetramine (HMT) or cetyltrimethylammonium bromide (CTAB) [19, 20]. In contrast, thermal spraying is capable of directly depositing photocatalytic and electrocatalytic coatings without any binder.

In view of the drawbacks of the conventional synthesis routes, it is of high interest to develop “greener” routes

for the preparation of photocatalysts while (i) avoiding tedious processes and the consumption/wastage of noxious chemicals and (ii) allowing faster and cost-effective production.

This is where thermal spraying can bring significant advantages owing to its simplicity and straightforwardness that enables the direct formation of films rather than noxious nanopowders, a key asset for the industrialization phase. Indeed, thermal spraying offers a rich set of technologies which deliver a large variety of coatings for the industry and have proved their high efficiency and versatility [21] in a large number of applications. Up to now, the thermal spraying processes are most often used to produce protective coatings and the works devoted to photocatalytic and electrocatalytic applications are rather scarce in the literature. Yet thermal spraying is capable to directly deposit binder-free photocatalytic and electrocatalytic coatings. More specifically, the relatively novel “solution precursor thermal spray” (SPTS) and “suspension thermal spray” (STS) processes which use aqueous solutions as feedstocks, offer flexible possibilities for depositing nanostructured films. Indeed, as shown later in this paper, nanostructuring is a key factor for high photocatalytic and electrocatalytic performances [21–23]. It is therefore timely to explore the capabilities of these techniques as potential options for the depollution and the storage of green energies.

The present review of the state-of-the-art works carried out in these fields is focused on presenting successively (i) the deposition principles of different thermal spraying techniques, (ii) some major developments and applications achieved in the fields of photocatalytic and electrocatalytic coatings.

## 2 Thermal spray processes for photocatalytic and electrocatalytic coatings

The concept of thermal spraying was created by Max Ulrich Schoop in 1910 in Zurich. Thermal spray processes comprise a family of coating technologies in which a stream of finely divided metals are deposited on a substrate, in a molten or semi-molten form, to form a continuous coating [21]. The thermal spray torch heats and melts the feedstock and accelerates the resulting particles towards the substrates, forming morphologies known as “splats” or “lamellar-structures” [21, 24, 25]. A schematic of this process is shown in Fig. 1. The final coatings can be built-up by depositing the feedstock material after a certain number of passes. The heated and accelerated droplets or particles are able to (i) plastically deform on impact and rapidly cool into thin lamellae; (ii) adhere to the surface, and (iii) overlap and interlock into a consolidated layer during the rapid solidification process [24]. Depending on the source of energy, thermal-spray

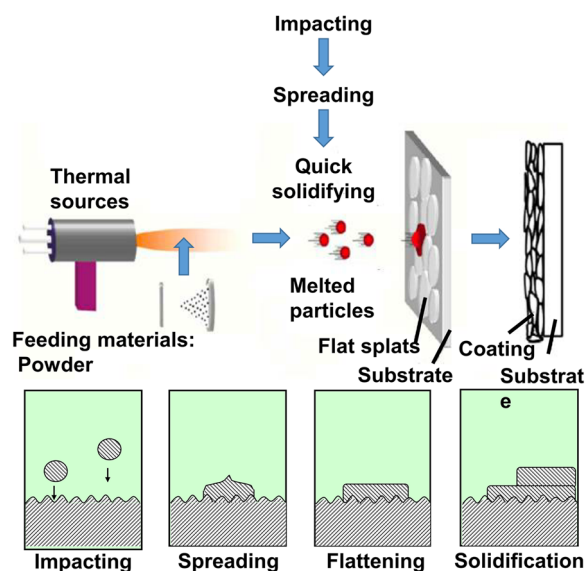


Fig. 1 Schematic of the thermal spray process [28]

processes can be categorized as combustion, electric arc and kinetic, as shown in Fig. 1 [24, 26]. Due to the roughness of substrate surface by sand-blasting and the rapid cooling procedure of each splat, the thermal sprayed, the basic bonding mechanism of thermal sprayed coatings is mechanical interlocking, where the bonding strength between splats can be improved by increasing temperature or particle velocities during particle impact on the substrates [27]. In the kinetic thermal spray (also called “cold spray”), the coatings are formed by way of the plastic deformation of ductile metallic or alloyed powders, which differs from combustion spraying or electrical-discharge plasma spraying [21]. Owing to the strong impact between particle and substrate, the kinetic energy of powder was converted into heat, and severe plastic deformation happened upon impact with the substrate. As a result, the bonding mechanism of cold sprayed coatings is combination of mechanical interlocking and metallurgical bonding [27]. In fact, the conventional low-pressure or high-pressure cold spraying is not suitable

for depositing ceramic materials that are materials of choice in photocatalytic and electrocatalytic applications. Therefore, the following presentation will concentrate on the combustion spray and electrical-discharge thermal spray routes.

### 2.1 Combustion spraying

Flame spraying is the oldest thermal-spray technology, characterized by low capital investment, high deposition rates and efficiencies, and relative ease of operation [29].

The high velocity oxy-fuel spray (HVOF) process is a new member of the family of combustion spraying techniques, which employs combustion energy from a gas or liquid fuel to heat the injected powders. A Laval-type nozzle is used to achieve high gas velocity (up to 2,000 m/s). The temperature of flame jet is in the range of 2500 °C to 3200 °C, relying on the type of fuel, the ratio of fuel gas/ oxygen as well as the gas pressure. Owing to the use of air instead of oxygen, high velocity air–fuel spray (HVOF) generates lower gas temperature and higher gas velocities than HVOF [21, 29]. The detonation gun (D-gun™) is similar to the HVOF devices, the difference being that the explosion of fuel and oxygen creates a detonation-pressure wave instead of the continuous steady state characteristic of the normal HVOF process [26]. However, the HVOF, HVOF and D-gun processes are characterized by high particle speeds and more energetic impacts on the substrate, leading to rather dense coatings. Especially, the IFKB lab—University of Stuttgart has been firstly develop the HVOF process with liquid feedstock, named as high-velocity suspension flame spraying (HVSFS) [30]. Moreover, comparing the coatings via HVOF technique, the HVSFS-deposited coatings are favorable for catalytic performances, such as the photo-degradation application, due to more anatase phase and higher porosity [31]. The schematic diagram of HVOF and HVSFS process in Fig. 2 [29, 31].

### 2.2 Conventional plasma spraying

Depending on the type of plasma, these devices involve both direct-current (DC) and radio-frequency (RF)

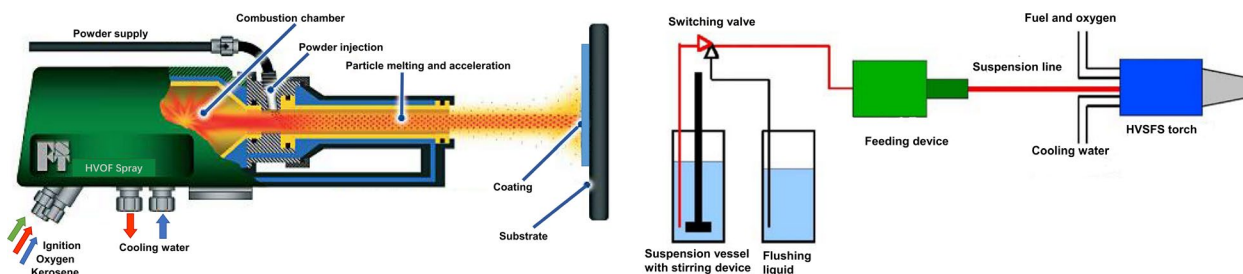


Fig. 2 Schematic diagram of high velocity oxy-fuel spray and high velocity suspension flame spraying system [29, 31]

inductively coupled plasma [26]. In DC-plasma spraying, an electric arc generates a plasma within a dedicated torch. The torch mainly comprised a tungsten cathode (usually a rod or of button-type design) and a cylindrical copper anode as the nozzle, which are cooled by water during the spray. The plasma gas is injected at the base of the cathode, heated by the arc, and exits the nozzle in the form of a high-temperature, high-velocity jet. The main gases used for DC plasma spray are Ar–H<sub>2</sub>, Ar–He–H<sub>2</sub>, N<sub>2</sub>–H<sub>2</sub> mixtures, resulting in a core temperature inside the plasma plume as high as 13,000K at the nozzle exit [21]. Figure 3 shows a schematic diagram of the DC-plasma spraying process. When the deposition is performed at atmospheric pressure, the process is commonly called atmospheric plasma spraying (APS). Currently, the torch power for the conventional APS system could be up to 50 kW, indicating possibly to melt and deposit all the materials in the earth. When it is under soft vacuum conditions, it is commonly referred to as vacuum plasma spraying (VPS), which helps avoiding external contaminations and limiting the formation of unwanted secondary phases in the coatings. Since the vacuum system is expensive, the gas shroud system has been also introduced in to the APS process to restrict the amount of entrained air and oxygen [26]. Generally, APS is used for depositing ceramic-based coatings due to the high temperature of the plasma plume, and the feedstock are normally in the form of powders of tens of micrometers size particles. For the conventional APS-deposited coatings, their characteristics mainly depending on the melting degree of particles. The states of particles inside of plasma jet could be controlled by the gas flow rate of primary gas and secondary gas, current of plasma torch, powder-feeding rate, as well as the spraying distance [32]. More recently, solution and suspension precursors as feedstock have been introduced to deposit finely structured films. The solution precursor plasma spray (SPPS) will be explored in more detail in the next section, since it proves to be one of the most appropriate processes to prepare porous, nanostructured films.

Another type of plasma, the RF inductively coupled plasma, is generated through the electromagnetic coupling of energy into a discharge cavity, is [21]. Like in the DC-plasma spray process, the atmosphere can be adjusted according to the targeted properties of the coatings. Compared to DC-plasma spraying, its greatest advantage is that it is well fitted for melting large particles of materials of low thermal conductivity [21]. However, this feature is not appropriate for the deposition of photocatalytic and electrocatalytic coatings, since the latter require high surface areas to maximize catalytic performances.

### 2.3 Liquid feedstock plasma spray (LFTS)

Nanoscale materials possess unique properties in view of photocatalytic and electrocatalytic applications [33]. In conventional plasma spray processes, the lamellae-structured coatings are formed by accumulated splats having diameters from a few tens to a few hundreds of micrometers [22]. Moreover, the major barrier faced when trying to deposit nanometer-size powders by normal thermal spraying is the difficulty of directly injecting very small particles into the high-temperature gas flow, since the momentum of the injected powder has to be of the same order as that imparted by the gas flow. In fact, it has been recognized that it is practically impossible to properly inject powder of sizes smaller than 5–10 μm [22].

This opened the question of how to form finely structured coatings, including nanostructured ones. An answer to that question was initiated in the mid-1990s with the introduction of the solution-precursor and suspension-based thermal sprays. Indeed, there are two possible routes for circumventing the drawback of the small particle size:

- (1) The solution precursor thermal spraying (SPTS), in which an aqueous or non-aqueous solution containing the cation(s) necessary to synthesize the desired oxide is fed into the high-temperature flame to form the final coating [21–23].

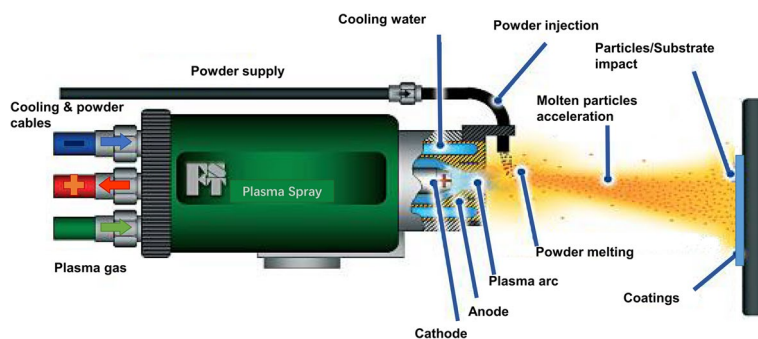


**Fig. 3** Schematic diagram of DC plasma spraying process [29]

- (2) The suspension thermal spraying, in which a suspension of nanometer-sized powders is injected with a liquid rather than with a carrier gas, the nanometer-sized powders being suspended inside the liquid phase (e.g. water or ethanol) by means of dispersants [21, 22].

As far as the solution precursor thermal spray (SPTS) process is concerned, the first attempts were conducted at the State University of New York in 1997 and 1998 [33–35], using common flames or DC-plasma torches. Since increasing attention was paid to thermal barrier coating (TBC) and solid-oxide fuel-cell (SOFC) applications [36, 37], the use of DC plasma torches have been improved to deposit suitable microstructures starting from solution precursors, giving rise to the “solution precursor plasma spray” (SPPS) technique. As reported by M. Gell and as illustrated in Fig. 4, once the solution precursor is injected into the plasma plume, each droplet undergoes a series of chemical and physical reactions within a single step, including the evaporation of the precursor solvent, droplet breakup, precursor-solute precipitation, pyrolysis, sintering, melting, and crystallization [38]. The results clearly showed that this new SPPS technique offers a fast and facile way to deposit finely structured metal oxide films from simple solution precursors. As shown in Fig. 4, the core temperature of the plasma plume can be as high as 13,000K, a suitable level for the instantaneous decomposition and pyrolysis of any metal salt into the corresponding metal oxide. In particular, for some complex compositions, containing e.g. two distinct metallic cations, there is a high probability for a direct synthesis and deposition of binary oxides. For example, perovskite  $\text{La}_{1-x}\text{Sr}_x\text{MnO}_3$  (LSM) [39] and  $\text{ZnFe}_2\text{O}_4$  spinel [40] coatings were easily obtained by the SPPS method. Furthermore, the nanocrystalline structuration of the SPPS-deposited coatings can be attributed to (1) the very

short flight time inside the ultrahigh-temperature plasma plume (in the order of milliseconds), which efficiently restricts the grain growth of the in-flight particles and (2) the extremely high cooling rate ( $10^6$  °C/min) during the deposition of the hot particles on the substrate [41].

As far as the suspension thermal spray is concerned, the DC plasma spray was the earliest route explored (1996) at the University of Sherbrook [42]; the technique was then termed the “suspension plasma spray” (SPS) route. Recently, the use of HOVF sprayed suspensions has been studied to produce wear-resistant and superhydrophobic coatings [43, 44]. Like in the SPPS route, the suspensions and the surrounding droplets experience multiple physical evolutions within the high-temperature of the hot plume created either by the plasma or the combustion, but without chemical reactions [22]. However, a disadvantage of suspension based thermal spray methods is that commercial or previously synthesized nanopowders are required, meaning extra costs to procure the raw nanomaterials, lower versatility in the selection of coating compositions, and possible health issues caused by the fine particles. Indeed, the major interest of the three novel technologies lies in the flexibility in adjusting the compositions and nanostructures of the aimed metal oxides. The accumulated experience has shown that the suspension-based route (using plasma or HOVF as spraying techniques) are less suitable for functional applications than the solution precursor thermal spray (SPTS) route. Due to the horizontal deposition route, the liquid feedstock thermal sprayed coatings normally exhibited less impact of particles onto the substrates, indicating higher porosity and lower mechanical properties. Besides, since the consumption of energy for evaporation of solvent from solution or suspension, the liquid feedstock thermal sprayed coatings also exhibited lower deposition efficiencies than the techniques with solid powder and wire feedstock [23].

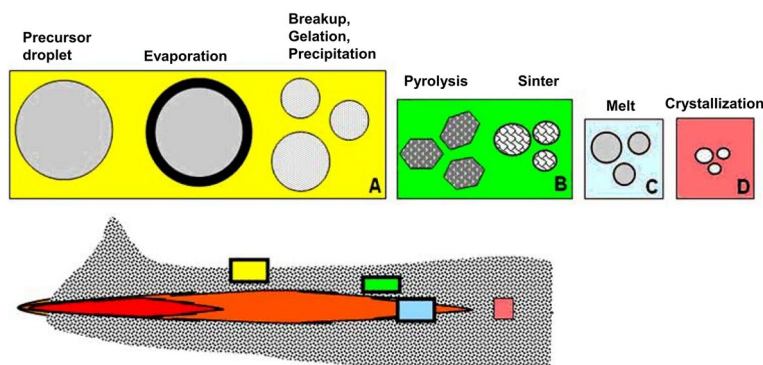


**Fig. 4** Chemical and physical evolution of a droplet injected into a plasma plume in SPPS process [38]

### 3 Interest of coatings deposited by thermal spray within photocatalytic and electrocatalytic applications

As stressed previously, thermal sprays techniques offer the key advantage of allowing a one-step formation of films within several minutes, in practical applications. Especially, solution precursor thermal spraying is a technique of choice to obtain tunable compositions and nanostructures, including more or less complex phases, starting simply from adequate aqueous solutions of metallic cations.

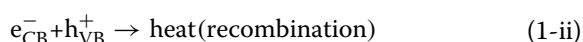
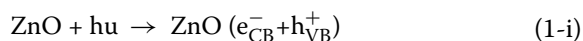
This paper section will set out the developments of thermal-sprayed photocatalytic and electrocatalytic coatings and evaluate their performances in these applications.

#### 3.1 Photocatalytic degradation of pollutants: The contribution of thermal spray coatings

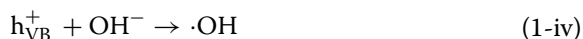
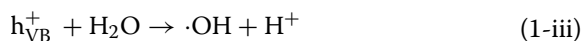
As early as 1976, the interest of the photocatalytic degradation of pollutants by TiO<sub>2</sub> was highlighted by John H. Carey [45] who found that various organic pollutants could be degraded and mineralized into small basic molecules, essentially H<sub>2</sub>O and CO<sub>2</sub>. This form of photocatalytic treatment, based on metal-oxide semiconductors, represents an ideal method to destroy aqueous pollutants by simply exploiting the inexhaustible solar energy without consuming any chemical reagents.

Taking ZnO as an example of photocatalyst active under suitable light irradiation, the relevant processes can be summarized as follows. At first, photogenerated electron-hole pairs are formed in the valance band. If the photon energy (hν) of the irradiation light is larger than the bandgap (E<sub>g</sub>) of ZnO, the electrons of the latter are excited and get transferred from the valance band (VB) to the conduction band (CB), leaving a positive hole in the

valence band. This first process is depicted by reaction 1-i and is denoted by a yellow dashed circle in Fig. 5 [46]. The electrons become then available to react with the pollutants that are contained in the water surrounding the photocatalyst. In competition with the charge transfers that enable these chemical reactions is the recombination of electrons and holes. This recombination effect is expressed by the reaction 1-ii and can occur within the volume of the MOS catalysts (as illustrated by the path A in Fig. 5) or at their surface (path B in Fig. 5), simultaneously releasing energy in the form of heat [47, 48].



Only the remaining available electrons (e<sup>-</sup>) and holes (h<sup>+</sup>) that succeed their separation up to the external surface of the ZnO particles (as illustrated by paths C and D in Fig. 5) will participate in the photocatalytic reactions. The holes in the valence band will thus react with surface-absorbed water molecules or absorbed hydroxyl groups (OH<sup>-</sup>) to form hydroxyl radicals (•OH) as illustrated in reactions 1-iii and 1-iv, respectively [48, 49].



On the other hand, conduction-band electrons will reduce surface-absorbed oxygen atoms to form primarily superoxide radical anions (O<sub>2</sub><sup>•-</sup>). In addition, during further steps of the photocatalytic process, other oxidizing radicals are formed, such as hydroperoxyl radical (HOO•), hydrogen peroxide (H<sub>2</sub>O<sub>2</sub>) and hydroxyl radicals (•OH)

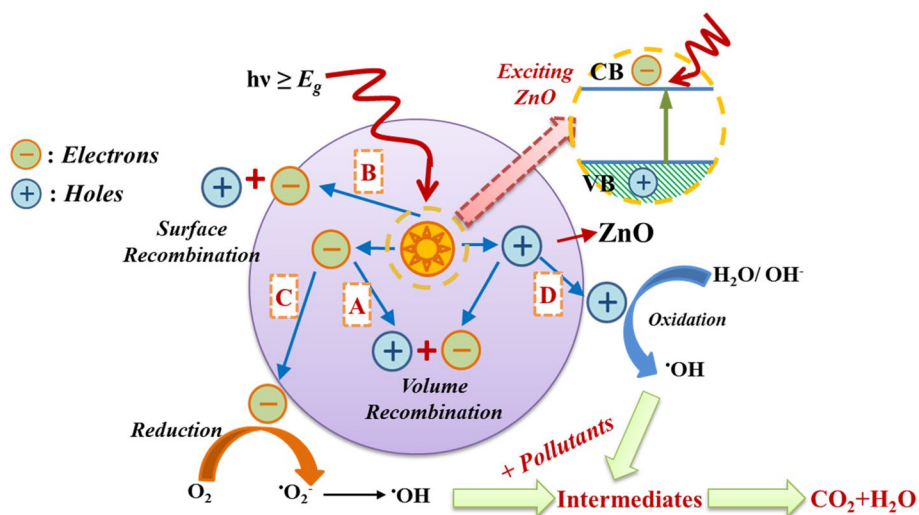
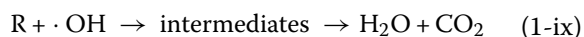
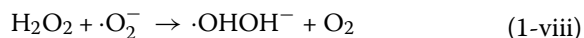


Fig. 5 Schematic of the working principle of a MOS (ZnO) photocatalysts

[47–50]. The corresponding processes (reactions 1-v, 1-vi, 1-vii and 1-viii) are summarized by the following reactions.



where R represents the organic compound.

Finally, due to its electrophilic nature (electron preferring), the hydroperoxyl radicals, such as  $\cdot OH$ , can non-selectively oxidize almost all electron rich organic molecules, eventually converting them to  $CO_2$  and water (as shown in reaction 1-ix) [47]. The organic pollutant is also degraded by photogenerated holes as some of its molecules are adsorbed on the MOS particles [49]. Finally, it must be mentioned that it is still not clear which of the aforementioned reaction pathways plays the most significant role, under given experimental conditions [51].

A search performed on the “Web of Science” indicates that a total of 31 articles have been issued so far on the photodegradation of organic dyes used as surrogates of pollutants using different thermal spray processes. Their photodegradation efficiency and the corresponding test conditions are shown in Table 1, except for the

**Table 1** Performances and test conditions for degradation of organic dyes based on the coatings deposited by different thermal spray routes

Materials	Pollutants	Light source	Irradiation time (min)	Degradation efficiency (%)	Deposition routes	Ref
ZnO	Orange II	UV	120	100	SPPS	[57]
		Vis	360	46.2		
CuO/ZnO	Orange II	UV	180	90	SPSS	[58]
CeO <sub>2</sub> -ZnO	Orange II	UV	240	100	SPPS	[59]
		Vis	360	62		
CuO/ZnO NR	Orang II	UV	300	98	SPPS	[60]
ZnFe <sub>2</sub> O <sub>4</sub>	Orange II	Vis	360	95	SPPS	[61]
TiO <sub>2</sub>	MB	UV	360	80	SPPS	[62]
TiO <sub>2</sub>	MB (12.8 μM)	UV	480	85.4	SPPS	[63]
Cu <sup>2+</sup> -TiO <sub>2</sub> (Scraped as powder)	MB (0.01 mM)	Visible	80	100	SPPS	[64]
TiO <sub>2</sub> -HA-rGO	MB (5 ppm)	UV	330	78	SFS	[65]
TiO <sub>2</sub> -HA	MB (5 ppm)	UV	330	94.2	SFS	[66]
TiO <sub>2</sub>	RhB (50 μM)	UV	360	76.4	HVSFS	[67]
TiO <sub>2</sub>	MB (5 mg/L)	UV	660	74	SPS	[68]
TiO <sub>2</sub>	MB (10 μM)	UV	180	~9	SPS	[69]
TiO <sub>2</sub>	MB (10 mg/L)	UV	100	66	APS	[70]
TiO <sub>2</sub> (PEC with $j_{anod} = 1 \text{ mA/cm}^2$ )	Orange II	Solar	180	70	APS	[17]
TiO <sub>2</sub> (PEC with $j_{anod} = 1 \text{ mA/cm}^2$ )	Orange II (15 mg/L)	Solar	120	98	APS	[71]
TiO <sub>2</sub>	MB (5 ppm)	UV	660	74	APS	[72]
TiO <sub>2</sub>	MB (5 ppm)	UV	900	84	APS	[73]
TiO <sub>2</sub>	MB (0.05 mM)	UV	120	27	APS	[74]
TiO <sub>2</sub>	MB (5 mg/L)	UV	180	24.2	APS	[75]
TiO <sub>2</sub>	MB (50 mg/L)	UV	2880	~38	HVOF	[76]
TiO <sub>2</sub> /CNTs	MB (0.01 mM)	UV	180	~37	APS	[53]
TiO <sub>2</sub>	MB (0.01 mM)	UV	90	64	HVOF	[77]
ZnO	MB (5 mg/L)	UV	180	~38	APS	[78]
Al doped ZnO	MB	UV-Vis	120	22.8	APS	[79]
ZnFe <sub>2</sub> O <sub>4</sub>	MB (5 mg/L)	Vis	180	30	FS	[80]
Fe <sub>2</sub> O <sub>3</sub>	MB (5 mg/L)	Vis	180	~23	FS	[81]
		UV	180	~13		

PEC Photoelectrocatalysis, MB Methylene blue, RhB Rhodamine B, SFS Suspension Flame Spray, HVSFS High Velocity Suspension Flame Spray, APS Air Plasma Spray with powders, FS Flame spray with powder

papers [52] to [53]. In the reference [54], the used  $\text{TiO}_2$  membrane proved virtually inactive since the result of the blank experiment was found very close to that of  $\text{TiO}_2$ . In addition, the testing device was unconventional, which raises a doubt whether some experimental artefacts produced the observed degradation effects. In [31, 55, 56], the necessary information about the photocatalytic degradation could not be found or calculated. For the photodegradation tests, the as-sprayed coatings with substrates were directly placed into a breaker or Petri dish containing organic pollutants. As such, it is feasible to do the cycling tests, without requirement of the post-filtration. Before irradiation, the liquid with samples was magnetically stirred for several hours in the dark to reach the adsorption–desorption equilibrium. During the subsequent light irradiation under room temperature, 1 mL of the liquid was extracted at regular time intervals to evaluate the remaining concentration of organic pollutants by measuring its UV–visible spectrum [57].

As shown in Table 1,  $\text{TiO}_2$  is the most studied material regardless of the spraying method used. Different photocatalytic degradation efficiencies might be related to different microstructures and film compositions as well as to different testing conditions. Except the single metal oxides (e.g.  $\text{TiO}_2$  and  $\text{ZnO}$ ), the doped metal oxides (e.g.  $\text{Co}^{3+}$  doped  $\text{ZnO}$ ), heterostructured metal oxides (e.g.  $\text{CuO}/\text{ZnO}$ ), as well as binary metal oxides ( $\text{ZnFe}_2\text{O}_4$ ) are interesting candidates as well, due to the narrowed bandgap and better separation of photogenerated holes and electrons [6, 52, 82]. For example, it can be seen that higher photodegradation activity was observed with  $\text{Cu}^{2+}$ - $\text{TiO}_2$  photocatalysts in [64] compared to other studies. It should be noted that the researchers ground the deposited films into a fine powder before the photocatalytic tests [64], which could be the reason for the improved performance owing to better interaction between the dye and the increased coating surface. This point was supported by [53, 70], where the finely powdered photocatalysts exhibited indeed better performance than photocatalysts produced with the same materials but in the form of coatings. However, another possible explanation for the improved performance obtained in [64] might be the formation of oxygen vacancies in the  $\text{Cu}$ -doped  $\text{TiO}_2$  films, which represents another possible means for enhancing the performances of e.g. SPPS sprayed coatings. The potential formation mechanism of oxygen vacancies from SPPS-sprayed coatings could be attributed to the typical non-equilibrium procedure and usage of reducing hydrogen gas during deposition. However, it should be mentioned that the post-heating treatment possibly to reduce the concentration of oxygen vacancies in the as-sprayed coatings [83].

Taking again  $\text{TiO}_2$  film as an example, Fig. 6 shows the morphologies produced via different spraying methods. Although different microstructures and different porosities can be expected from using different deposition routes, all the coatings were still composed of conventional flattened splats and irregular particles, meaning low surface area and consequently limited activity. Furthermore, in the APS-deposited  $\text{ZnO}$  coatings [79], the higher intensity of the X Ray diffraction signal was observed for the (101) crystallographic planes and the lower intensity for the (002) planes. This can be related to a general morphology which is not well nanostructured. Indeed, as shown in Fig. 6, all these samples seemed to be devoid of: 1) particle nanostructures (e.g. nanorods, nanowires, and nanoflakes); 2) hierarchical morphologies; and 3) preferential exposure of most active crystal planes (002). It was then suspected that SPPS route could provide better results owing to its capability of depositing hierarchical metal-oxide films with well-shaped nanostructures along with the preferential exposure of the most active crystallographic planes to the solution.

In addition, the relationships that exist between the porosity, the surface roughness and the film thickness on the one hand and the photodegradation efficiency on another hand have been investigated [17, 74]. Higher porosity and larger surface roughness induce larger contact area between the MOS and the solution, resulting in better photocatalytic performance. However, as illustrated in [17], there is actually a loose correlation between the photocatalytic degradation of organic pollutants on the one hand and the porosity as well as the coating thickness on another hand. In addition, during the APS-deposition experiments  $\text{TiO}_2$  that set out in [74], the most porous  $\text{TiO}_2$  coating was obtained using the lowest spraying power (16 kW), while the best performance was obtained for the depositions performed at the 20 kW (medium) spraying power. Finally, the porosities (i.e. the volume porosities) were calculated based on cross-section images of the coatings and included therefore the inner pores that are inaccessible and thus inoperative within photocatalytic processes. One can then infer that the coating thickness has in fact virtually no influence on the final performance. In other words, injecting lower quantities of precursors to form less thick films with better performance appeared as the preferable strategy. Another important aspect is that the performance of the photocatalytic can be limited by the wettability of the active films. This suggests that hydrophobic surfaces instead of hydrophilic ones are preferable [62].

Furthermore, for the most studied  $\text{TiO}_2$  coatings, they could be composed by anatase and rutile phases, where



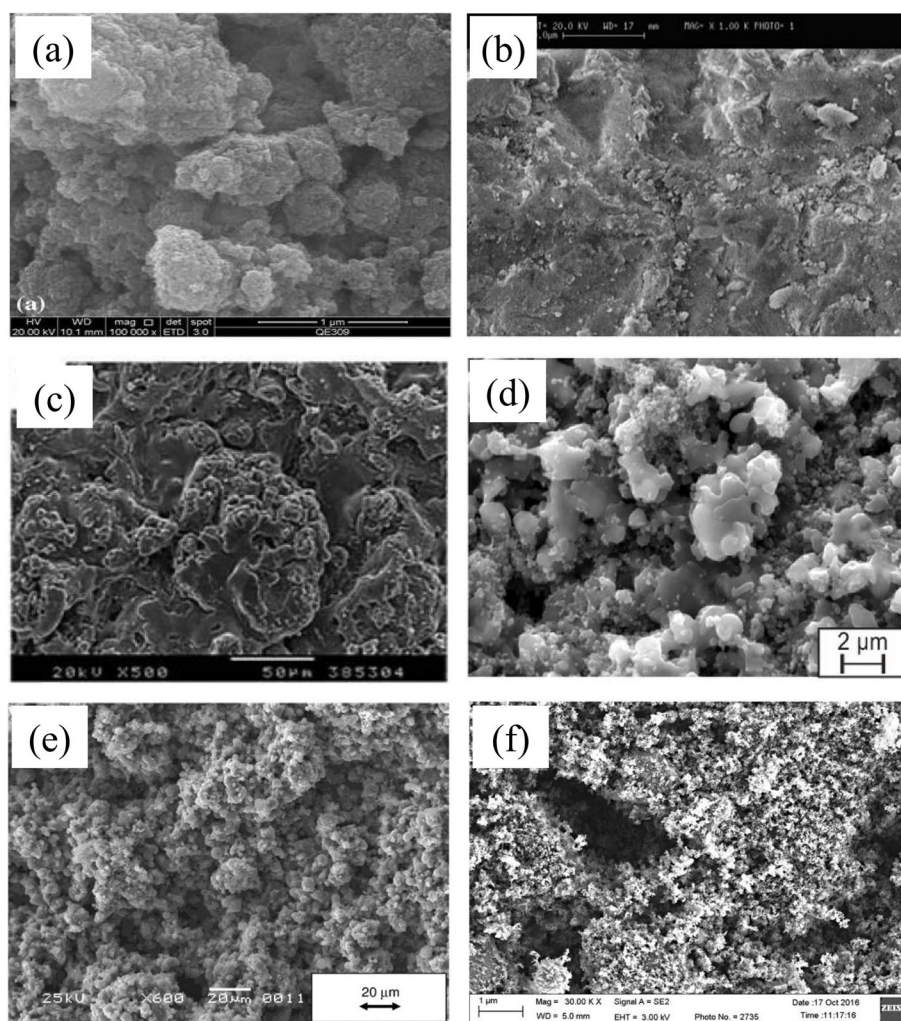


**Fig. 6** Surface morphologies of  $\text{TiO}_2$  films deposited by (a) SFS [66], (b) HVOF [77], (c) APS [17], (d) HVSFS [67], (e) SPS [69] and (f) SPPS [63] routes

the anatase phase is metastable. For the  $\text{TiO}_2$  coatings deposited by various thermal spraying techniques, the P25/20 powders were employed with the anatase ratio from 75 vol.% to 80 vol.% [31, 84–86]. Especially, for the solution precursor thermal spraying techniques, the organic salts were employed as liquid feedstock, named as titanium isopropoxide ( $\text{Ti}(\text{OCH}(\text{CH}_3)_2)_4$ ). It was found that photocatalytic performances of  $\text{TiO}_2$  coatings are sensitive to the phase composition, where higher anatase phase improve the photocatalytic activities. The phase composition of  $\text{TiO}_2$  coatings was generally sensitive to the melting degree of the particles during spraying, where the rutile phase correspond to the fully melted particles, and the anatase structure was mostly present in the partially and non-melted particles. It was found that anatase ratio is mainly affected by the different thermal spraying sources and feedstock, where lower heating source and liquid feedstock (e.g. suspension and precursor solution)

are more favorable for anatase composition [31, 84, 85]. Besides, the spraying distances, torch power, solution concentration determines the phase composition of  $\text{TiO}_2$  coatings as well [31, 86, 87]. All in all, the liquid feedstock thermal spraying techniques, including SPPS, SPS and HVSFS, could be more favorable for the photocatalytic  $\text{TiO}_2$  coatings, thanks to the more porous surface morphologies, finer structures and higher ratio of anatase phase.

$\text{ZnO}$  is another promising photocatalyst for photodegradation, exhibiting similar bandgap structure to  $\text{TiO}_2$ . Comparing with  $\text{TiO}_2$ ,  $\text{ZnO}$  also benefits from the following advantages: 1)  $\text{ZnO}$  is the ability to absorb a wide range of solar spectrum and more light quanta than some semiconducting [48], 2) Its various precursors were commonly inorganic salts, which are highly soluble in many solvents and highly versatile with respect to the formation of different hierarchical structures [88]. By contrast,

the precursors for  $\text{TiO}_2$  were mostly organic metal salts, which are not only more expensive but more difficult to prepare due to the need for hydrolysis [48, 89]. Therefore, we decided to orient our efforts towards the development of novel hierarchical nanostructures in ZnO related coatings by using the solution precursor plasma spray (SPPS) technique as deposition technique. As shown in Fig. 7, the SPPS-deposited ZnO coatings exhibited hierarchical microstructures consisting in sea-urchin and aloe-vera like nanoparticles, developing high surface areas and efficiently exposing high activity crystal planes [90]. In the work program that was then conducted, we investigated the effect of the solute type and water pH value on the surface morphologies of SPPS-deposited ZnO coatings and we observed a high potential of that approach to form novel microstructures [90]. The brand-new hierarchical nanostructures (including nanorods and nanowires) did enhance the efficiency of photodegradation that reached 100% after 120 min irradiation [57]. In addition, owing to the far-from-equilibrium conditions that prevail in plasma sprays and the further usage of hydrogen to create oxygen vacancies, we obtained highly oxygen-defective ZnO coatings which exhibited photodegradation performance even under visible light (46.2% after 360 min irradiation). This can be attributed to the narrowing of the MOS bandgap caused by the creation of oxygen vacancies [57]. Besides, in order to improve the photocatalytic activities under visible light, the heterostructured and binary metal oxides photocatalysts were also studied

by SPPS techniques, where the metallic nitrates were used as the precursor solute due to their better solubility. For the heterostructured photocatalysts, we studied the CuO-ZnO, MnO-ZnO,  $\text{CeO}_2$ -ZnO,  $\text{Fe}_2\text{O}_3$ -ZnO and  $\text{Co}_3\text{O}_4$ -ZnO heterostructures based on the SPPS process [58–60]. In these works, we endeavored to optimize the phase composition ratios in the synthesized photocatalytic coatings and we studied the influence of laminated architectures and nanorods morphologies on the photocatalytic performances [58–60]. For example, the use of the  $\text{CeO}_2$ -ZnO system enabled to substantially increase the photodegradation efficiency which reached 62% after 360 min of irradiation under visible light [59]. It is worth stressing that it is the first time – to the authors' knowledge – that hierarchical nano-heterostructured films including ZnO such as those shown in Fig. 7 were obtained via the SPPS route [60]. For further improving the photodegradation performances under visible light, coatings of  $\text{ZnFe}_2\text{O}_4$  spinel have also been deposited and tested. It was found that such  $\text{ZnFe}_2\text{O}_4$  films display improved the activity under visible light, with degradation performances of the dye climbing up to 95% within 360 min, which is more than 2 times the level of the performances of pure ZnO samples [61].

In summary, the SPPS deposition route enables the production of hierarchical nanostructures and complex phase compositions with tunable composition ratios, leading to enhanced photodegradation performances both under UV and visible light conditions.

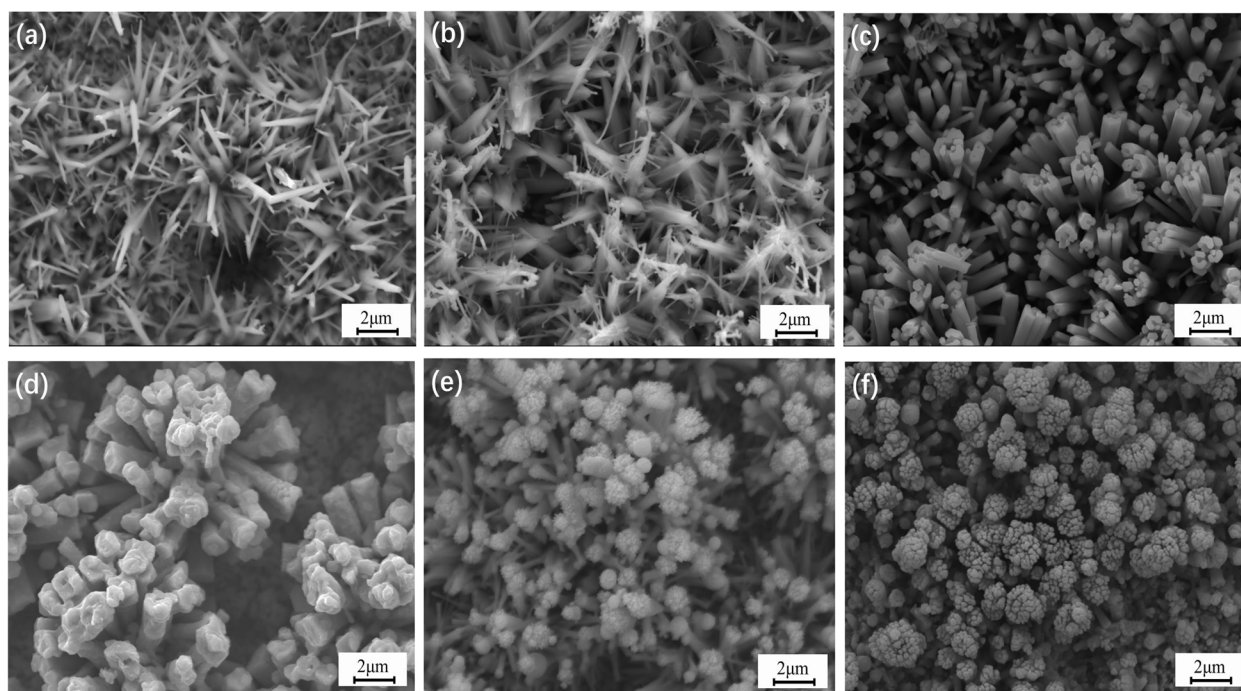


**Fig. 7** Novel hierarchical nanostructures of SPPS-deposited ZnO and ZnO based heterostructured coatings. [60, 90]

### 3.2 Supercapacitor electrodes: The contribution of thermal spray coatings

Supercapacitors, also known as electrochemical electric-energy storage devices, are mainly composed of two electrode materials, two current collectors, one separator (ion conductor) and an electrolyte, as shown in Fig. 8 [91]. The essential difference between a supercapacitor and a conventional parallel-plate capacitor is the presence in the former of a solid or liquid electrolyte between the two electrodes, which is the source of ions during its energy storage process. Since the electrode material plays a decisive role in the energy storage capacity of a supercapacitor, many studies have focused on the preparation and improvement of such materials.

Depending on the energy storage mechanism, supercapacitors can be classified as electric double-layer capacitors (EDLCs) or pseudocapacitors. In EDLCs, the charge is stored by way of the surface adsorption of ions from the electrolyte as a result of electrostatic attraction, which leads to the formation of two charged layers (the so-called double layer). The EDLC charge-storage mechanism is depicted in Fig. 9a. When the EDLC is charged, owing to the external circuit, cations contained in the electrolyte concentrate on the negative electrode whilst anions concentrate on the positive one, forming an EDL that compensates for the external charge imbalance. In the process of discharging, electrons travel from the negative to the positive electrode via an external circuit and both types of ions in the pores intermingle again until the cell is discharged [7]. The maximum capacitance of an EDLSC is controlled by the surface area of its active electrode and its pore-size distribution to typical values, reaching 0.15–0.4 F/m<sup>2</sup> or ~150 F/g1 for carbon [92]. Conway first introduced the “pseudocapacitor” in the 1970s, using electrosorption, reduction–oxidation (redox) reactions, and intercalation processes [93, 94].

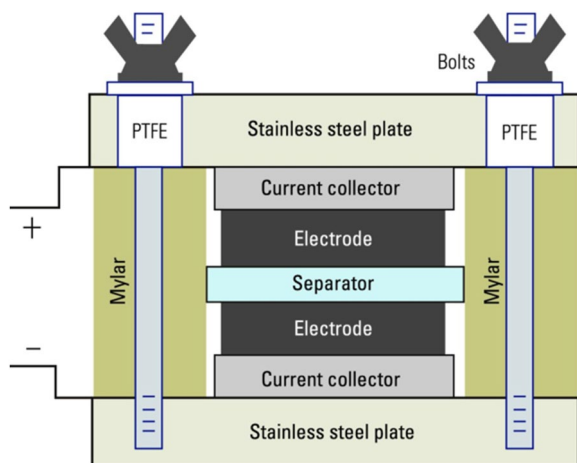


Fig. 8 The schematic diagram of supercapacitors. [91]

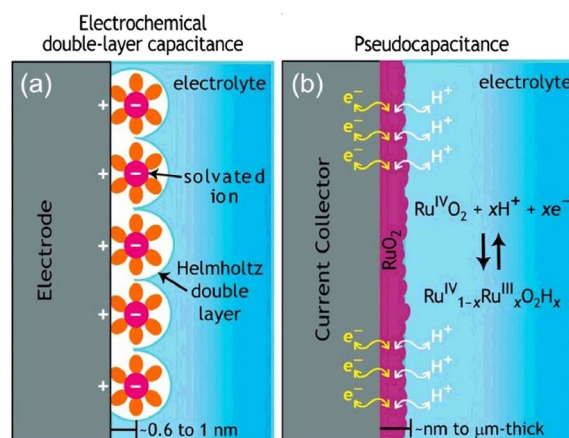


Fig. 9 Schematic diagram of storage mechanisms of charges in (a) EDLCs and (b) pseudocapacitance. [98]

Taking the RuO<sub>2</sub> electrode as an example, its corresponding mechanism of charge storage based on reversible redox reactions within a pseudocapacitor device is illustrated by Fig. 9b. When charging, the H<sup>+</sup> ions present in the electrolyte diffuse towards the electrode/liquid interface, driven by the external electric field, leading to reversible electrochemical reactions with the active materials (such as RuO<sub>2</sub>) on or near the surface. The H<sup>+</sup> can further penetrate into the bulk of RuO<sub>2</sub> during the above-mentioned redox reactions, resulting in the storage of a large amount of charges within the active materials. During the discharge, this stored charge is released as a current through the external circuit and the H<sup>+</sup> ions return to the electrolyte solution [95]. Table 2 lists several types of charge storage reactions that occur on metal oxide electrodes of pseudocapacitors [92]. It should be noted that pseudocapacitors must feature both a double layer capacitance and a fastly reversible, superficial redox reaction, which determine the energy density while maintaining fast charge and discharge times comparable to those of EDLCs [96, 97]. Moreover, owing to the surface and bulk properties of the active materials that are used in the electrodes involved in these redox reactions, the specific capacitances of pseudocapacitors can be 10–100 times those of EDLCs. In view of the above advantages, more attention and research is being paid to pseudocapacitors.

Supercapacitor seems a fairly new topic in the sphere of thermal spray applications, since only seven publications were found. Among these articles, five were based on the SPPS route [83, 99–102] and the remaining dealt with carbon-containing electrodes that were prepared using a conventional plasma-spray methods [103, 104]. Again, it is worth reminding that the thermal spray routes benefit from rapid, one-step synthesis of binder-free films, especially when one uses the SPPS process.

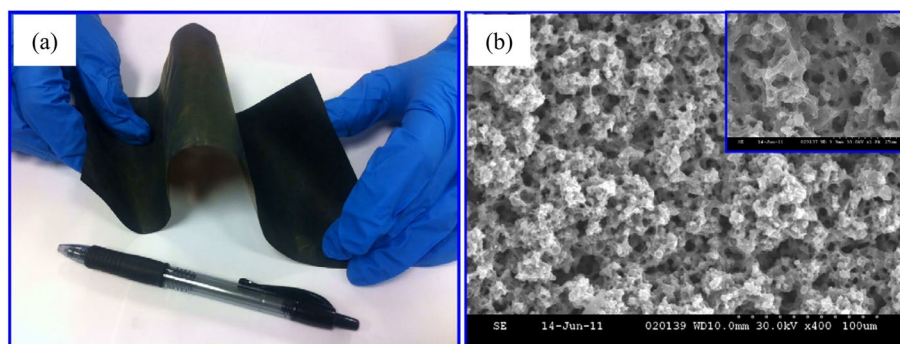
**Table 2** Several kind charge storage reactions based on metal oxide electrodes in the pseudocapacitors [92]

Electrodes	Electrolytes	Charge storage reaction
MnO <sub>2</sub>	Na <sub>2</sub> SO <sub>4</sub>	MnO <sub>2</sub> + Na <sup>+</sup> + e <sup>-</sup> = NaMnO <sub>2</sub>
NiO	KOH, NaOH	NiO + OH <sup>-</sup> = NiOOH + e <sup>-</sup>
Co <sub>3</sub> O <sub>4</sub>	KOH, NaOH	Co <sub>3</sub> O <sub>4</sub> + OH <sup>-</sup> + H <sub>2</sub> O = 3CoOOH + e <sup>-</sup> CoOOH + OH <sup>-</sup> = CoO <sub>2</sub> + H <sub>2</sub> O + e <sup>-</sup>
V <sub>2</sub> O <sub>5</sub>	NaCl, Na <sub>2</sub> SO <sub>4</sub>	V <sub>2</sub> O <sub>5</sub> + 4Na <sup>+</sup> + 4e <sup>-</sup> = Na <sub>2</sub> V <sub>2</sub> O <sub>5</sub>
RuO <sub>2</sub> ·xH <sub>2</sub> O	H <sub>2</sub> SO <sub>4</sub> , Na <sub>2</sub> SO <sub>4</sub>	RuO <sub>2</sub> + xH <sup>+</sup> + xe <sup>-</sup> = RuO <sub>2-x</sub> (OH) <sub>x</sub> (0 < x < 2)

Regarding the SPPS-deposited electrodes for supercapacitor applications, the University of Toronto first studied the use of MoO<sub>3</sub> coatings as electrode material, where the ammonium molybdate tetrahydrate was used as the precursor [100]. It was found that the specific capacitance of MoO<sub>3</sub> coatings decreased from 6.5 to 1.5 mF/cm<sup>2</sup> when the stand-off spraying distance increased from 55 to 155 mm, which was ascribed to different morphologies of the resulting films. Based on this study, M. Golzar [101] further developed molybdenum nitride (Mo<sub>2</sub>N) coatings by reacting in a tubular furnace some MoO<sub>3</sub> with a H<sub>2</sub>:N<sub>2</sub> (5:1 ratio) gas mixture and pure ammonia (NH<sub>3</sub>). The electrochemical tests demonstrated a capacitance of 4.1 mF/cm<sup>2</sup> for MoO<sub>3</sub>, while a much larger capacitance of 31 mF/cm<sup>2</sup> was found for Mo<sub>2</sub>N under the sweep rate of 100 mV/s. During that period, nanostructured Co<sub>3</sub>O<sub>4</sub> coatings were also developed via the SPPS process from the cobalt acetate tetrahydrate aqueous solution by University of Michigan [99]. The flexible Co<sub>3</sub>O<sub>4</sub> electrode was deposited on a current collector made by a stainless-steel sheet (SS304). Figure 10 and Fig. 10b displaying the microstructures of these Co<sub>3</sub>O<sub>4</sub> coatings that featured a specific capacitance of ~162 F g<sup>-1</sup> with a retention capacity of 72.2% after 1,000 cycles under a specific current rate of 2.75 A g<sup>-1</sup> in 6 M KOH electrolyte. The plasma-sprayed carbon coatings exhibited a specific capacity of only 15 F/g that was obtained when the specific surface

area of carbon powders was 577 m<sup>2</sup>/g [103]. This limited capacitance was likely due to the inherent limitations of carbon materials compared to metal oxides, as mentioned in Sect. 1.3.2. This point was further confirmed by a further work on a NiO/Carbon electrode, which reached 53.6 F/g as its highest specific capacitance [104].

The authors also did some research work on supercapacitor electrode coatings deposited via the solution precursor thermal spraying (SPTS) techniques. Hollow micro-/nanostructures and oxygen vacancies are highly desirable for supercapacitors as they both increase the active surface area and enhance electrochemical properties, respectively. In order to benefit from both effects, pioneering investigations were conducted on SPTS-deposited NiCo<sub>2</sub>O<sub>4</sub> coatings featuring hollow microspheres and high density of oxygen defects were. The NiCo<sub>2</sub>O<sub>4</sub> coatings were deposited from the nickel nitrate and cobalt nitrate precursor solution. As reported in previous papers [105], surface precipitation promotes the formation of hollow particles or shell structures. This is confirmed by the Fig. 11a that illustrates the result of one of our works [71]. The electrochemical testing clearly shows that the specific capacitances enhanced and multiplied by about 20 when using oxygen-deficient NiCo<sub>2</sub>O<sub>4</sub> electrodes containing hollow microspheres rather than NiCo<sub>2</sub>O<sub>4</sub> electrodes composed by solid particles devoid of oxygen vacancies. Figure 11a shows indeed that the NiCo<sub>2</sub>O<sub>4</sub> coatings composed of hollow spheres and featuring oxygen-vacancies develop a specific capacitance as high as 902 F/g at the current density of 1 A/g with a good retention of 89.2% after 2500 cycles under 20 mV/s scan rate. Based on this work, we elaborated Co<sub>3</sub>O<sub>4</sub> coatings with different densities of oxygen vacancies and particles shapes and tested them as supercapacitor electrode materials [83]. Both cobalt nitrate and cobalt acetate precursor solution were sprayed for these Co<sub>3</sub>O<sub>4</sub> coatings. We found that the films composed of submicron porous spheres and containing the highest content of

**Fig. 10** a Photograph of the current collector of an SPPS-deposited, flexible Co<sub>3</sub>O<sub>4</sub> electrode on a stainless steel sheet (SS304); b SEM of a Co<sub>3</sub>O<sub>4</sub> electrode films (inset—zoom in the view). [99]

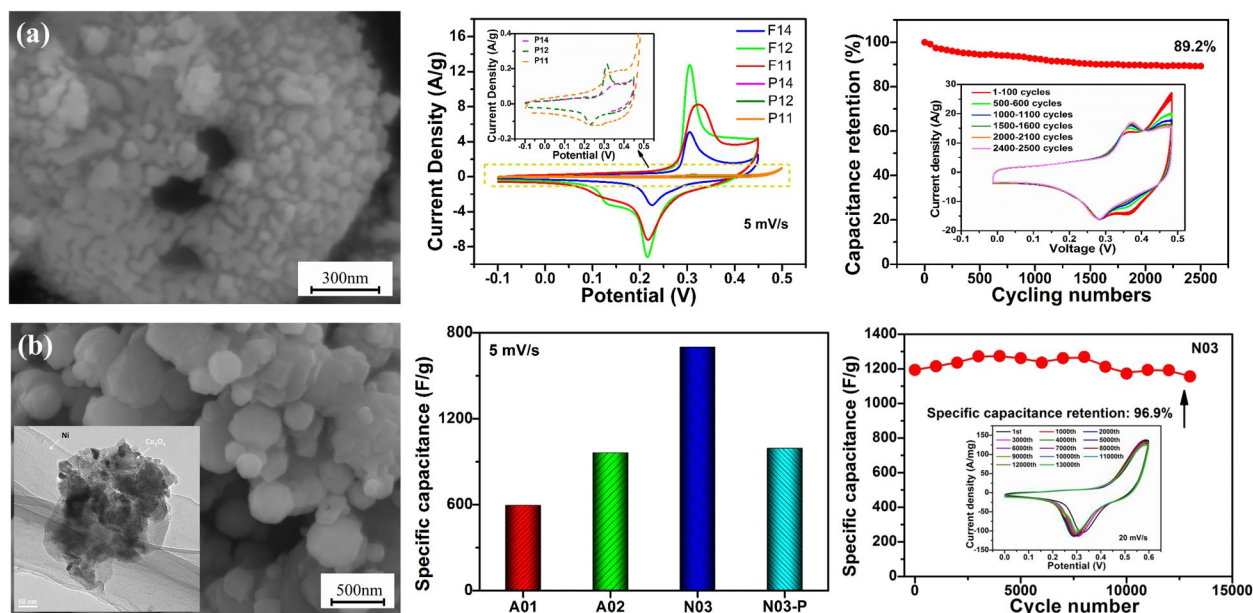


**Fig. 11** Surface morphologies and electrochemical performances of SPTS-deposited (a)  $\text{Ni}_2\text{O}_4$  and (b)  $\text{Co}_3\text{O}_4$  supercapacitor electrodes. [102]

oxygen vacancies exhibited specific capacitances as high as 1700 F/g under the scan rate of 5 mV/s. By contrast, after a heating post treatment, this value dropped down to 994 F/g due to the loss of the oxygen vacancies. Meanwhile, 96.9% of the initial capacitance was maintained after 13,000 consecutive cycles at a scan rate of 20 mV/s, as shown in Fig. 11b.

In summary, starting from a review of the literature, some original works that we carried out in our laboratory have confirmed the high potential of SPTS as a technique to prepare supercapacitor electrodes exhibiting very high capacitances. These high performances are rendered possible by the favorable surface morphologies and nanostructures as well as high densities of oxygen vacancies that are created by the plasma spray techniques, especially the STPS route.

Overall, although the liquid feedstock thermal spraying techniques exhibited high potential for depositing photocatalytic and electrocatalytic coatings with fine structures, they still met several limitations. Firstly, the as-sprayed material systems are still limited to the simple metal oxides, where the composites, other metal compounds (e.g. metal sulfides, metal nitrides) and high-entropy or medium-entropy materials were lack of studies. Secondly, the novel hierarchical microstructures with well-shaped nanostructures (e.g. nanorods, nanowires) were still waiting for expanding from ZnO related coatings to other materials. Besides, the deep understanding of the influence of coating characteristics on the coating performances should be strengthened, which could supply

guidance for further optimization of catalytic coatings via thermal spraying techniques. In addition, the liquid feedstock thermal sprayed coatings generally exhibited lower mechanical properties than conventional thermal spraying methods, where the higher adhesion and cohesion of coatings will be required for the industrial promotion with higher stability.

#### 4 Summary and prospects

This paper has provided a review of the uses of thermal spray techniques for the preparation of photocatalytically and electrocatalytically active coatings involving metal oxide semiconductors and intended for photodegradation of aqueous organic pollutants and the design of supercapacitors. It also integrates original results generated in this laboratory using more specifically the SPTS technique. Regarding the photodegradation of aqueous pollutants, the most studied materials are  $\text{TiO}_2$  and ZnO based coatings, for which the existing literature reports rather weak photocatalytic activities, especially under visible light, due to the wide bandgaps of these oxides when they are involved as defect-free, large crystallites. Indeed, photocatalytic coatings deposited by usual thermal spray methods are devoid of the favorable structural properties that are of 1) well defined nanostructures, e.g. nanorods or nanowires; 2) hierarchical morphologies and 3) preferential exposure of the most active crystal planes to the aqueous medium. On the contrary, the SPTS route enables the creation of brand-new hierarchical nanostructures and composite oxide phases with tunable compositions, which greatly improves

the photodegradation performances. However, further research efforts are necessary to make thermal sprayed coating a popular deposition technique of photocatalysts for the degradation of pollutants and to potentially reach the same performance levels as powdery photocatalysts, which are not environmentally, and health compatible. In the authors' opinion, some challenges were left 1) a systematic study of the hierarchical morphologies of MOS materials as this knowledge is currently limited to ZnO based coatings, 2) the coupling of different metal oxide superconductors likely to reduce the electron/hole recombination while exhibiting at the same time well defined nanostructures.

As far as supercapacitor electrodes are concerned, the literature reveals few research works involving thermal spray deposition methods, namely because the demand for supercapacitors is relatively recent. However, most of the works identified employ solution precursor thermal spraying (SPTS) techniques. This is probably due to the strong need, in this field, of fine structures and complex phase compositions to obtain good storage performances. Here again, The SPTS route proves highly interesting for preparing supercapacitor electrodes in the form of binder-free MOS films, as it is capable of not only generating suitable surface morphologies but also creating numerous oxygen vacancies.

At the light of the present review, these challenges were still waiting for investigation for the thermal sprayed supercapacitor electrode coatings: 1) one might investigate other advanced materials rather than simple metal oxides, limited by the low electric conductivities, 2) one should gain a better understanding of the relation between electrocatalytic coatings and supercapacitor performances to orient the research towards the most suitable structures.

In summary, thermal spraying techniques own promising assets for the elaboration of highly performing photocatalytic and electrocatalytic coatings. This is especially the case for the recently developed solution precursor thermal spray route. These assets are not only in terms of the favorable compositions and nanostructures they create but also in terms of industrialization prospects, thanks to the binder-free nature and the fast and single-step fabrication process.

#### Acknowledgements

The authors would like to acknowledge the project supported by the Natural Science Foundation of Jiangsu Higher Education Institution of China (Grant No. 20KJB430003), the open project of Key Laboratory of Green Fabrication and Surface Technology of Advanced Metal Materials (Grant No. GFST2021KF01), and Humboldt Fellowship for Postdoctoral Researcher (Dr. Zexin YU).

#### Authors' contributions

All authors read and approved the final manuscript.

## Declarations

#### Competing interests

The authors declare that they have no known competing financial interests or personal relationships that could have appeared to influence the work reported in this paper.

Received: 27 August 2023 Revised: 4 December 2023 Accepted: 7 December 2023

Published online: 04 February 2024

## References

- Hachem C, Bocquillon F, Zahraa O, Bouchy M (2001) Decolourization of textile industry wastewater by the photocatalytic degradation process. *Dyes Pigment* 49:117–125
- Ollis DF, Al-Ekabi H (1993) Elsevier Science Ltd
- Cai Z, Sun Y, Liu W, Pan F, Sun P, Fu J (2017) An overview of nanomaterials applied for removing dyes from wastewater. *Environ Sci Pollut Res* 24:15882–15904
- Zhao J, Burke AF (2021) Review on supercapacitors: Technologies and performance evaluation *Journal of Energy Chemistry* 59:276–291
- Miller JR, Simon P (2008) Electrochemical capacitors for energy management. *Science Magazine* 321:651–652
- Casbeer E, Sharma VK, Li X-Z (2012) Synthesis and photocatalytic activity of ferrites under visible light: a review. *Sep Purif Technol* 87:1–14
- González A, Goikolea E, Barrena JA, Mysyk R (2016) Review on supercapacitors: Technologies and materials. *Renew Sustain Energy Rev* 58:1189–1206
- Dubal DP, Gomez-Romero P, Sankapal BR, Holze R (2015) Nickel cobaltite as an emerging material for supercapacitors: An overview. *Nano Energy* 11:377–399
- Sk MM, Yue CY, Ghosh K, Jena RK (2016) Review on advances in porous nanostructured nickel oxides and their composite electrodes for high-performance supercapacitors. *J Power Sources* 308:121–140
- Nithya V, Arul NS (2016) Review on  $\alpha$ -Fe<sub>2</sub>O<sub>3</sub> based negative electrode for high performance supercapacitors. *J Power Sources* 327:297–318
- Cui L, Li J, Zhang X-G (2009) Preparation and properties of Co<sub>3</sub>O<sub>4</sub> nanorods as supercapacitor material. *J Appl Electrochem* 39:1871
- Xing W, Li F, Yan Z-F, Lu G (2004) Synthesis and electrochemical properties of mesoporous nickel oxide. *J Power Sources* 134:324–330
- Tang W, Liu L, Tian S, Li L, Yue Y, Wu Y, Zhu K (2011) Aqueous supercapacitors of high energy density based on MoO<sub>3</sub> nanoplates as anode material. *Chem Commun* 47:10058–10060
- Hsu C-T, Hu C-C (2013) Synthesis and characterization of mesoporous spinel NiCo<sub>2</sub>O<sub>4</sub> using surfactant-assembled dispersion for asymmetric supercapacitors. *J Power Sources* 242:662–671
- Pu J, Wang J, Jin X, Cui F, Sheng E, Wang Z (2013) Porous hexagonal NiCo<sub>2</sub>O<sub>4</sub> nanoplates as electrode materials for supercapacitors. *Electrochim Acta* 106:226–234
- Dey NK, Kim MJ, Kim K-D, Seo HO, Kim D, Kim YD, Lim DC, Lee KH (2011) Adsorption and photocatalytic degradation of methylene blue over TiO<sub>2</sub> films on carbon fiber prepared by atomic layer deposition. *J Mol Catal A: Chem* 337:33–38
- Dosta S, Robotti M, Garcia-Segura S, Brillas E, Cano IG, Guilemany JM (2016) Influence of atmospheric plasma spraying on the solar photoelectro-catalytic properties of TiO<sub>2</sub> coatings. *Appl Catal B* 189:151–159
- Wang H-J, Sun Y-Y, Wang C-F, Cao Y (2012) Controlled synthesis, cytotoxicity and photocatalytic comparison of ZnO films photocatalysts supported on aluminum matrix. *Chem Eng J* 198:154–162
- Ali AM, Emanuelsson EA, Patterson DA (2010) Photocatalysis with nanostructured zinc oxide thin films: The relationship between morphology and photocatalytic activity under oxygen limited and oxygen rich conditions and evidence for a Mars Van Krevelen mechanism. *Appl Catal B* 97:168–181

20. Ni Y-H, Wei X-W, Ma X, Hong J-M (2005) CTAB assisted one-pot hydrothermal synthesis of columnar hexagonal-shaped ZnO crystals. *J Cryst Growth* 283:48–56
21. Fauchais PL, Heberlein JVR, Boulos MI (2014) Thermal spray fundamentals: from powder to part. Springer Science & Business Media
22. Fauchais P, Vardelle A (2012) Advanced Plasma Spray Applications, InTech
23. Jordan EH, Jiang C, Gell M (2015) The solution precursor plasma spray (SPPS) process: a review with energy considerations. *J Therm Spray Technol* 24:1153–1165
24. Ang ASM, Sanpo N, Sesso ML, Kim SY, Berndt CC (2013) Thermal spray maps: material genomics of processing technologies. *J Therm Spray Technol* 22:1170–1183
25. Li C-J, Ohmori A (2002) Relationships between the microstructure and properties of thermally sprayed deposits. *J Therm Spray Technol* 11:365–374
26. Gan JA, Berndt CC (2015) Thermal spray forming of titanium and its alloys. *Titanium Powder Metallurgy* 425–446
27. Li C-J, Luo X-T, Yao S-W, Li G-R, Li C-X, Yang G-J (2022) The bonding formation during thermal spraying of ceramic coatings: a review. *J Therm Spray Technol* 31:780–817
28. Li C-J (2010) Thermal spraying of light alloys. Aluminium, Magnesium and Titanium Alloys Woodhead Publishing Series in Metals and Surface Engineering. *Surface Engineering of Light Alloys* 184–241
29. Amin S, Panchal H (2016) A review on thermal spray coating processes, transfer, 2
30. Killinger A, Kuhn M, Gadow R (2006) High-velocity suspension flame spraying (HVSFS), a new approach for spraying nanoparticles with hypersonic speed. *Surf Coat Technol* 201:1922–1929
31. Bolelli G, Cannillo V, Gadow R, Killinger A, Lusvardi L, Rauch J (2009) Properties of high velocity suspension flame sprayed (HVSFS) TiO<sub>2</sub> coatings. *Surf Coat Technol* 203:1722–1732
32. Lynam A, Romero AR, Xu F, Wellman R, Hussain T (2022) Thermal spraying of ultra-high temperature ceramics: A review on processing routes and performance. *J Therm Spray Technol* 31:745–779
33. Karthikeyan J, Berndt C, Tikkanen J, Wang J, King A, Herman H (1997) Nanomaterial powders and deposits prepared by flame spray processing of liquid precursors. *Nanostruct Mater* 8:61–74
34. Karthikeyan J, Berndt CC, Reddy S, Wang JY, King AH, Herman H (1998) Nanomaterial deposits formed by DC plasma spraying of liquid feedstocks. *J Am Ceram Soc* 81:121–128
35. Karthikeyan J, Berndt C, Tikkanen J, Wang J, King A, Herman H (1997) Preparation of nanophase materials by thermal spray processing of liquid precursors. *Nanostruct Mater* 9:137–140
36. Jordan EH, Xie L, Gell M, Padture N, Cetegen B, Ozturk A, Ma X, Roth J, Xiao T, Bryant P (2004) Superior thermal barrier coatings using solution precursor plasma spray. *J Therm Spray Technol* 13:57–65
37. Padture N, Schlichting K, Bhatia T, Ozturk A, Cetegen B, Jordan E, Gell M, Jiang S, Xiao T, Strutt P (2001) Towards durable thermal barrier coatings with novel microstructures deposited by solution-precursor plasma spray. *Acta Mater* 49:2251–2257
38. Gell M, Jordan EH, Teicholz M, Cetegen BM, Padture NP, Xie L, Chen D, Ma X, Roth J (2008) Thermal barrier coatings made by the solution precursor plasma spray process. *J Therm Spray Technol* 17:124–135
39. Wang Y, Coyle T (2011) Solution Precursor Plasma Spray of Porous La<sub>1-x</sub>Sr<sub>x</sub>MnO<sub>3</sub> Perovskite Coatings for SOFC Cathode Application. *J Fuel Cell Sci Technol* 8:021005
40. Dom R, Sivakumar G, Hebalkar NY, Joshi SV, Borse PH (2012) Deposition of nanostructured photocatalytic zinc ferrite films using solution precursor plasma spraying. *Mater Res Bull* 47:562–570
41. Singh V, Karakoti A, Kumar A, Saha A, Basu S, Seal S (2010) Precursor dependent microstructure evolution and nonstoichiometry in nanostructured cerium oxide coatings using the solution precursor plasma spray technique. *J Am Ceram Soc* 93:3700–3708
42. Ravi B, Sampath S, Gambino R, Parise J, Devi P (2006) Plasma spray synthesis from precursors: Progress, issues, and considerations. *J Therm Spray Technol* 15:701–707
43. Bai M, Kazi H, Zhang X, Liu J, Hussain T (2018) Robust hydrophobic surfaces from suspension HVOF thermal sprayed rare-earth oxide ceramics coatings. *Sci Rep* 8:6973
44. Murray J, Ang A, Pala Z, Shaw E, Hussain T (2016) Suspension high velocity oxy-fuel (SHVOF)-sprayed alumina coatings: microstructure, nanoindentation and wear. *J Therm Spray Technol* 25:1700–1710
45. Carey JH, Lawrence J, Tosine HM (1976) Photodechlorination of PCB's in the presence of titanium dioxide in aqueous suspensions. *Bull Environ Contam Toxicol* 16:697–701
46. Herrmann J-M (1999) Heterogeneous photocatalysis: fundamentals and applications to the removal of various types of aqueous pollutants. *Catal Today* 53:115–129
47. Chong MN, Jin B, Chow CW, Saint C (2010) Recent developments in photocatalytic water treatment technology: a review. *Water Res* 44:2997–3027
48. Lee KM, Lai CW, Ngai KS, Juan JC (2016) Recent developments of zinc oxide based photocatalyst in water treatment technology: a review. *Water Res* 88:428–448
49. Uddin MT (2013) Second-ary Metal oxide heterostructures for efficient photocatalysts, Université Sciences et Technologies-Bordeaux I
50. Dionysiou DD, Khodadoust AP, Kern AM, Suidan MT, Baudin I, Lainé J-M (2000) Continuous-mode photocatalytic degradation of chlorinated phenols and pesticides in water using a bench-scale TiO<sub>2</sub> rotating disk reactor. *Appl Catal B* 24:139–155
51. Agustina TE, Ang HM, Vareek VK (2005) A review of synergistic effect of photocatalysis and ozonation on wastewater treatment. *J Photochem Photobiol, C* 6:264–273
52. Low J, Yu J, Jaroniec M, Wageh S, Al-Ghamdi AA (2017) Heterojunction photocatalysts. *Adv Mater* 29:1601694
53. Daram P, Banjongprasert C, Thongsuwan W, Jiansirisomboon S (2016) Microstructure and photocatalytic activities of thermal sprayed titanium dioxide/carbon nanotubes composite coatings. *Surf Coat Technol* 306:290–294
54. Lin Y-F, Tung K-L, Tzeng Y-S, Chen J-H, Chang K-S (2012) Rapid atmospheric plasma spray coating preparation and photocatalytic activity of macroporous titania nanocrystalline membranes. *J Membr Sci* 389:83–90
55. Bozorgtabar M, Rahimipour M, Salehi M (2010) Novel photocatalytic TiO<sub>2</sub> coatings produced by HVOF thermal spraying process. *Mater Lett* 64:1173–1175
56. Toma F-L, Berger L, Jacquet D, Wicky D, Villaluenga I, de Miguel Y, Lindeløv J (2009) Comparative study on the photocatalytic behaviour of titanium oxide thermal sprayed coatings from powders and suspensions. *Surf Coat Technol* 203:2150–2156
57. Yu Z, Moussa H, Ma Y, Liu M, Chouchene B, Schneider R, Moliere M, Liao H (2019) Oxygen-defective ZnO films with various nanostructures prepared via a rapid one-step process and corresponding photocatalytic degradation applications. *J Colloid Interface Sci* 534:637–648
58. Yu Z, Moussa H, Liu M, Schneider R, Wang W, Moliere M, Liao H (2019) Development of photocatalytically active heterostructured MnO/ZnO and CuO/ZnO films via solution precursor plasma spray process. *Surf Coat Technol* 371:107–116
59. Yu Z, Chouchene B, Liu M, Moussa H, Schneider R, Moliere M, Liao H, Chen Y, Sun L (2020) Influence of laminated architectures of heterostructured CeO<sub>2</sub>-ZnO and Fe<sub>2</sub>O<sub>3</sub>-ZnO films on photodegradation performances. *Surf Coat Technol* 403:126367
60. Yu Z, Moussa H, Liu M, Schneider R, Moliere M, Liao H (2019) Heterostructured metal oxides-ZnO nanorods films prepared by SPPS route for photodegradation applications. *Surf Coat Technol* 375:670–680
61. Yu Z, Moussa H, Chouchene B, Liu M, Schneider R, Wang W, Moliere M, Liao H (2018) One-step synthesis and deposition of ZnFe<sub>2</sub>O<sub>4</sub> related composite films via SPPS route for photodegradation application. *Nanotechnology* 30:045707
62. Kindole D, Ando Y (2017) Application of atmospheric solution precursor plasma spray to photocatalytic devices for small and medium industries in developing countries. *Japanese Journal of Applied Physics* 56:01AB10
63. Solonenko O, Ando Y, Nishiyama H, Kindole D, Smirnov A, Golovin A, Uehara S, Nakajima T (2018) Synthesis of thick photocatalytic titania surface layers by solution plasma spraying and subsequent treatment by pulsed laminar plasma jet. *Surf Coat Technol* 333:39–51
64. R. Kumar, S. Govindarajan, R.K. Siri Kiran Janardhana, T.N. Rao, S.V. Joshi, S (2016). Anandan, Facile one-step route for the development of in situ cocatalyst-modified Ti<sup>3+</sup> self-doped TiO<sub>2</sub> for improved visible-light photocatalytic activity, *ACS appl mater interfaces*. 8:27642–27653
65. Huang J, Gong Y, Liu Y, Suo X, Li H (2017) Developing titania-hydroxyapatite-reduced graphene oxide nanocomposite coatings

- by liquid flame spray deposition for photocatalytic applications. *J Eur Ceram Soc* 37:3705–3711
66. Liu Y, Huang J, Ding S, Liu Y, Yuan J, Li H (2013) Deposition, characterization, and enhanced adherence of *Escherichia coli* bacteria on flame-sprayed photocatalytic titania-hydroxyapatite coatings. *J Therm Spray Technol* 22:1053–1062
  67. Toma F-L, Berger L-M, Shakhverdova I, Leupolt B, Potthoff A, Oelschlägel K, Meissner T, Gomez JAI, de Miguel Y (2014) Parameters influencing the photocatalytic activity of suspension-sprayed TiO<sub>2</sub> coatings. *J Therm Spray Technol* 23:1037–1053
  68. Liu X, Wen K, Deng C, Yang K, Deng C, Liu M, Zhou K (2018) Nanostructured Photocatalytic TiO<sub>2</sub> Coating Deposited by Suspension Plasma Spraying with Different Injection Positions. *J Therm Spray Technol* 27:245–254
  69. Kozerski S, Toma F-L, Pawlowski L, Leupolt B, Latka L, Berger L-M (2010) Suspension plasma sprayed TiO<sub>2</sub> coatings using different injectors and their photocatalytic properties. *Surf Coat Technol* 205:980–986
  70. Yi Z, Guofeng C, Ma W, Wei W (2008) Effect of external bias voltage and coating thickness on the photocatalytic activity of thermal sprayed TiO<sub>2</sub> coating. *Prog Org Coat* 61:321–325
  71. Garcia-Segura S, Dosta S, Guilemany JM, Brillas E (2013) Solar photoelectrocatalytic degradation of Acid Orange 7 azo dye using a highly stable TiO<sub>2</sub> photoanode synthesized by atmospheric plasma spray. *Appl Catal B* 132:142–150
  72. Bordes MC, Vicent M, Moreno A, Moreno R, Borrell A, Salvador M, Sánchez E (2013) Microstructure and photocatalytic activity of APS coatings obtained from different TiO<sub>2</sub> nanopowders. *Surf Coat Technol* 220:179–186
  73. Bordes MC, Vicent M, Moreno A, López V, Moreno R, Benavente R, Sánchez E (2014) Preparation of feedstocks from nano/submicron-sized TiO<sub>2</sub> particles to obtain photocatalytic coatings by atmospheric plasma spraying. *Ceram Int* 40:16213–16225
  74. Zhang C, Chaudhary U, Das S, Godavarty A, Agarwal A (2013) Effect of Porosity on Photocatalytic Activity of Plasma-Sprayed TiO<sub>2</sub> Coating. *J Therm Spray Technol* 22:1193–1200
  75. Bordes MC, Vicent M, Moreno R, García-Montaña J, Serra A, Sánchez E (2015) Application of plasma-sprayed TiO<sub>2</sub> coatings for industrial (tannery) wastewater treatment. *Ceram Int* 41:14468–14474
  76. Colmenares-Angulo J, Zhao S, Young C, Orlov A (2009) The effects of thermal spray technique and post-deposition treatment on the photocatalytic activity of TiO<sub>2</sub> coatings. *Surf Coat Technol* 204:423–427
  77. Bozorgtabar M, Salehi M, Rahimpour M, Jafarpour M (2010) Influence of high velocity oxy-fuel parameters on properties of nanostructured TiO<sub>2</sub> coatings. *Bull Mater Sci* 33:671–675
  78. Navidpour A, Kalantari Y, Salehi M, Salimijazi H, Amirnasr M, Rismanchian M, Siahkali MA (2017) Plasma-Sprayed Photocatalytic Zinc Oxide Coatings. *J Therm Spray Technol* 26:717–727
  79. Su C, Lu C, Hsiao W, Liu W, Shieu F (2013) Evaluation of the microstructural and photocatalytic properties of aluminum-doped zinc oxide coatings deposited by plasma spraying. *Thin Solid Films* 544:170–174
  80. Navidpour A, Salehi M, Salimijazi H, Kalantari Y, Siahkali MA (2017) Photocatalytic Activity of Flame-Sprayed Coating of Zinc Ferrite Powder. *J Therm Spray Technol* 26:2030–2039
  81. Navidpour A, Salehi M, Amirnasr M, Salimijazi H, Siahkali MA, Kalantari Y, Mohammadnezhad M (2015) Photocatalytic Iron Oxide Coatings Produced by Thermal Spraying Process. *J Therm Spray Technol* 24:1487–1497
  82. Samadi M, Zirak M, Naseri A, Khorashadizade E, Moshfegh AZ (2016) Recent progress on doped ZnO nanostructures for visible-light photocatalysis. *Thin Solid Films* 605:2–19
  83. Yu Z, Ma Y, Liu M, Huang X, Song C, Song G, Liao H, Chen Y, Sun L (2021) Oxygen-deficient Co<sub>3</sub>O<sub>4</sub> submicron porous sphere films as highly active supercapacitor electrodes. *Surf Coat Technol* 405:126513
  84. Bozorgtabar M, Rahimpour M, Salehi M (2010) Effect of thermal spray processes on anatase–rutile phase transformation in nano-structured TiO<sub>2</sub> photo-catalyst coatings. *Surf Eng* 26:422–427
  85. Toma F-L, Sokolov D, Bertrand G, Klein D, Coddet C, Meunier C (2006) Comparison of the photocatalytic behavior of TiO<sub>2</sub> coatings elaborated by different thermal spraying processes. *J Therm Spray Technol* 15:576–581
  86. Lee C, Choi H, Lee C, Kim H (2003) Photocatalytic properties of nanostructured TiO<sub>2</sub> plasma sprayed coating. *Surf Coat Technol* 173:192–200
  87. Simfroso K, Cabo SR, Unabia R, Britos A, Sokolowski P, Candidato R Jr (2023) Solution Precursor Plasma Spraying of TiO<sub>2</sub> Coatings Using a Catalyst-Free Precursor. *Materials* 16:1515
  88. Kumar SG, Rao KK (2015) Zinc oxide based photocatalysis: tailoring surface-bulk structure and related interfacial charge carrier dynamics for better environmental applications. *RSC Adv* 5:3306–3351
  89. Daneshvar N, Salari D, Khataee A (2004) Photocatalytic degradation of azo dye acid red 14 in water on ZnO as an alternative catalyst to TiO<sub>2</sub>. *J Photochem Photobiol, A* 162:317–322
  90. Yu Z, Moussa H, Liu M, Chouchene B, Schneider R, Wang W, Moliere M, Liao H (2018) Tunable morphologies of ZnO films via the solution precursor plasma spray process for improved photocatalytic degradation performance. *Appl Surf Sci* 455:970–979
  91. Wu Z-S, Feng X, Cheng H-M (2014) Recent advances in graphene-based planar micro-supercapacitors for on-chip energy storage. *Natl Sci Rev* 1:277–292
  92. Zhi M, Xiang C, Li J, Li M, Wu N (2013) Nanostructured carbon–metal oxide composite electrodes for supercapacitors: a review. *Nanoscale* 5:72–88
  93. Simon P, Gogotsi Y, Dunn B (2014) Where do batteries end and supercapacitors begin? *Science* 343:1210–1211
  94. Augustyn V, Simon P, Dunn B (2014) Pseudocapacitive oxide materials for high-rate electrochemical energy storage. *Energy Environ Sci* 7:1597–1614
  95. Long JW, Bélanger D, Brousse T, Sugimoto W, Sassin MB, Crosnier O (2011) Asymmetric electrochemical capacitors—Stretching the limits of aqueous electrolytes. *MRS Bull* 36:513–522
  96. Wang G, Zhang L, Zhang J (2012) A review of electrode materials for electrochemical supercapacitors. *Chem Soc Rev* 41:797–828
  97. Jost K, Dion G, Gogotsi Y (2014) Textile energy storage in perspective. *Journal of Materials Chemistry A* 2:10776–10787
  98. Zhang X, Cheng X, Zhang Q (2016) Nanostructured energy materials for electrochemical energy conversion and storage: A review. *J Energy Chem* 25:967–984
  99. Tummala R, Guduru RK, Mohanty PS (2012) Nanostructured Co<sub>3</sub>O<sub>4</sub> electrodes for supercapacitor applications from plasma spray technique. *J Power Sources* 209:44–51
  100. Golozar M, Chien K, Coyle TW (2012) Orthorhombic α-MoO<sub>3</sub> Coatings with Lath-Shaped Morphology Developed by SPPS: Applications to Super-Capacitors. *J Therm Spray Technol* 21:469–479
  101. Golozar M, Chien K, Lian K, Coyle TW (2013) Pseudo-Capacitors: SPPS Deposition and Electrochemical Analysis of α-MoO<sub>3</sub> and Mo<sub>2</sub>N Coatings. *J Therm Spray Technol* 22:710–722
  102. Ma Y, Yu Z, Liu M, Song C, Huang X, Moliere M, Song G, Liao H (2019) Deposition of binder-free oxygen-vacancies NiCo<sub>2</sub>O<sub>4</sub> based films with hollow microspheres via solution precursor thermal spray for supercapacitors. *Ceram Int* 45:10722–10732
  103. Kavaliauskas Ž, Marcinauskas L, Aikas M, Valinčius V, Milieška M, Baltušnikas A (2017) Effect of carbon powder thermal activation on characteristics of supercapacitor electrodes. *J Electrostat* 90:61–66
  104. Kavaliauskas Z, Marcinauskas L, Valatkevicius P (2011) Formation and characterization of carbon and nickel oxide/carbon composites for supercapacitors. *Acta Phys Pol, A* 119:253–255
  105. Saha A, Seal S, Cetegen B, Jordan E, Ozturk A, Basu S (2009) Thermo-physical processes in cerium nitrate precursor droplets injected into high temperature plasma. *Surf Coat Technol* 203:2081–2091

## Publisher's Note

Springer Nature remains neutral with regard to jurisdictional claims in published maps and institutional affiliations.